Expert Systems with Applications 38 (2011) 6190–6201

Contents lists available at ScienceDirect

Expert Systems with Applications

journal homepage: www.elsevier.com/locate/eswa

Wavelet basis functions in biomedical signal processing

J. Rafiee [a,*], M.A. Rafiee [a], N. Prause [b], M.P. Schoen [c]

[a] Department of Mechanical, Aerospace and Nuclear Engineering, Rensselaer Polytechnic Institute, Troy, NY 12180, USA
[b] The Mind Research Network, 1101 Yale Blvd. NE, Albuquerque, NM 87106, USA
[c] Measurement and Control Engineering Research Center, College of Engineering, Idaho State University, Pocatello, ID 83201, USA

ARTICLE INFO

Keywords:
Biomedical signal processing
Prosthetics
Myoelectric control
Psychophysiology
Mother wavelet
EMG
EEG
VPA
Pattern recognition
Daubechies (db 44)

ABSTRACT

During the last two decades, wavelet transform has become a common signal processing technique in various areas. Selection of the most similar mother wavelet function has been a challenge for the application of wavelet transform in signal processing. This paper introduces Daubechies 44 (db44) as the most similar mother wavelet function across a variety of biological signals. Three-hundred and twenty four potential mother wavelet functions were selected and investigated in the search for the most similar function. The algorithms were validated by three categories of biological signals: forearm electromyographic (EMG), electroencephalographic (EEG), and vaginal pulse amplitude (VPA). Surface and intramuscular EMG signals were collected from multiple locations on the upper forearm of subjects during ten hand motions. EEG was recorded from three monopolar Ag–AgCl electrodes (Pz, POz, and Oz) during visual stimulus presentation. VPA, a useful source for female sexuality research, were recorded during a study of alcohol and stimuli on sexual behaviors. In this research, after extensive studies on mother wavelet functions, results show that db44 has the most similarity across these classes of biosignals.

Published by Elsevier Ltd.

1. Introduction

Biosignal processing has been rapidly developing, increasing the understanding of complex biological processes in a wide variety of areas. Wavelet transform (Daubechies, 1991) is a powerful time-frequency approach which has been applied to multiple domains of biosignal processing, such as EMG (e.g. Englehart, Hudgins, & Parker, 2001), EEG (e.g. Kurt, Sezgin, Akin, Kirbas, & Bayram, 2009; Rosso et al., 2001; Subasi, 2005; Ting, Guo-zheng, Bang-hua, & Hong, 2008), ECG (e.g. Engin, Fedakar, Engin, & Korurek, 2007; Manikandan & Dandapat, 2008; Singh & Tiwari, 2006), VPA (e.g. Rafiee, Rafiee, & Michaelsen, 2009). A significant focus on the application of wavelet transforms (e.g. Englehart et al., 2001; Farina, Lucas, & Doncarli, 2008) has permitted rapid development in the field. However, the selection of the most appropriate mother wavelet to characterize commonalities amongst signals within a given domain is still lacking in biosignal processing. The main contributions to find the optimum basis function can be found in several papers (e.g. Brechet, Lucas, Doncarli, & Farina, 2007; Farina, do Nascimento, Lucas, & Doncarli, 2007; Flanders, 2002; Landolsi, 2006; Lucas, Gaufriau, Pascual, Doncarli, & Farina, 2008; Rafiee & Tse, 2009; Singh & Tiwari, 2006; Tse, Yang, & Tam, 2004).

The mother wavelet function is the main base of wavelet transforms that would permit identification of correlated coefficients across multiple signals. The more similar the mother wavelet function is to the wavelet coefficients across signals, the more precisely the signal of interest can be identified and isolated; hence, identification of a mother wavelet function is of paramount significance.

The Daubechies (db) wavelet functions (Daubechies, 1988) have been applied in several areas with the lower orders (db1 to db20) used most often (Rafiee & Tse, 2009). The few peer-reviewed papers about the application of higher order db refer to Antonino-Daviu, Riera-Guasp, Folch, and Palomares (2006) and Rafiee and Tse (2009) who implemented them for mechanical systems.

This paper focuses on the most similar wavelet basis function matched with complex biosignals such as surface and intramuscular EMG, EEG, and VPA signals (Rafiee, Rafiee, et al., 2009).

2. Measures

2.1. Surface and intramuscular EMG signals

EMG signals have broad applications in various areas, especially in prosthetics and myoelectric control (Asghari Oskoei & Hu, 2007). The experimental surface and intramuscular EMG signals used in this research have been provided from the Institute of Biomedical Engineering at the University of New Brunswick with a protocol approved by the university's Research Ethics Board (Hargrove, Englehart, & Hudgins, 2007). Two different data acquisition

* Corresponding author. Address: Department of Mechanical, Aerospace and Nuclear Engineering, Jonsson Engineering Center, Rm. 2049, 110 8th Street, Troy, NY 12180-3590, USA. Tel.: +1 518 276 6351; fax: +1 518 276 6025.
E-mail addresses: rafiee@rpi.edu, krafiee81@gmail.com (J. Rafiee).

0957-4174/$ - see front matter Published by Elsevier Ltd.
doi:10.1016/j.eswa.2010.11.050

systems were used to collect surface and intramuscular EMG signals (Hermens et al., 1999). For surface EMG signals, a 16-electrode linear array with interelectrode spacing of 2 cm was used. Each channel was filtered between 10 and 500 Hz and amplified with a gain of 2000. For intramuscular EMG, needles were implanted in the pronator and supinator teres, flexor digitorum sublimas, extensor digitorum communis, flexor and extensor carpi ulnaris. These were used to record information regarding grip, wrist flexion and rotation, and gross movement. These six channels of data were filtered between 10 and 3000 Hz and also amplified with a gain of 2000. These were recorded in six subjects while they performed 10 hand movements for 5 s each, followed by a 2 min resting period. All subjects denied fatigue during these exercises. The location of surface and needle electrodes is depicted in Fig. 1 in a cross section of the forearm. The motions includes forearm pronation, forearm supination, wrist flexion, wrist extension, wrist abduction, wrist adduction, key grip, chuck grip, hand open, and a rest state.

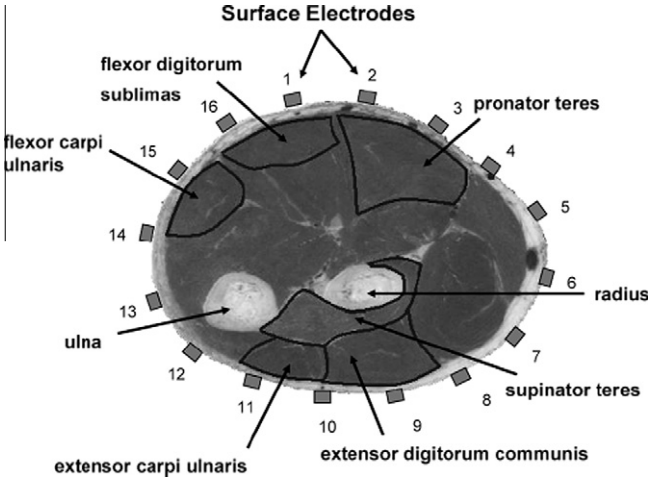

Fig. 1. A cross section of the upper forearm to illustrate the locations of 16 surface electrodes and six needle electrodes. *Source*: Hargrove, Englehart, & Hudgins, 2007, with permission.

2.2. EEG signals

EEG signals, one of the most complicated biomedical signals, are the variations of electrical potential in the cortex caused by the neuronal activity reflected in electrical potentials at the scalp. EEG offers high time-resolution for changes in mental and physical activity occurring in the brain and has been an investigative tool in such disparate areas as neuroprosthetics, affective psychopathology, diagnosis of nervous diseases, and cognitive models of learning. To illustrate the difference between EEG and EMG signals, their frequency contents are depicted using power spectrum density (see Figs. 2 and 3).

Neuroscan STIM software (Compumedics, Inc.) was used to collect EEG signals, present digitized emotional photographs, and collect physiological data. The EEG signals were recorded from three monopolar Ag–AgCl electrodes which were placed over three midline sites (Pz, POz, and Oz) for the purpose of recording visual evoked potentials (see Fig. 4). These locations were chosen to represent visual cortex and provide redundancy. All three-channel analogue EEG signals were converted to digital format through an A/D converter with a sampling rate of 300 Hz, and then amplified by 5000 using a Sensorium, Inc. EPA-6 bioamplifier. The signals were then filtered using a high-pass filter at 10 Hz (12 dB/Octave) and a low-pass filter at 30 Hz (eighth order elliptic). Impedance was maintained below 10 kΩ by thorough skin preparation, including abrasion. EEG signals recorded in this research have the applications to investigate the relationship of emotion and attention to sexual stimuli and participants' sexual desire levels (Prause, Janssen, & Hetrick, 2007). Participants were seated in a chair and viewed standardized photographs that varied systematically in their emotional content (International Affective Picture System; Center for the Study of Emotion and Attention, 1995). Each stimulus was presented for 6 s with a variable (M = 13 s) inter-trial interval. For the current study, only the data recorded from one subject was used. While spectral density can vary due to individual

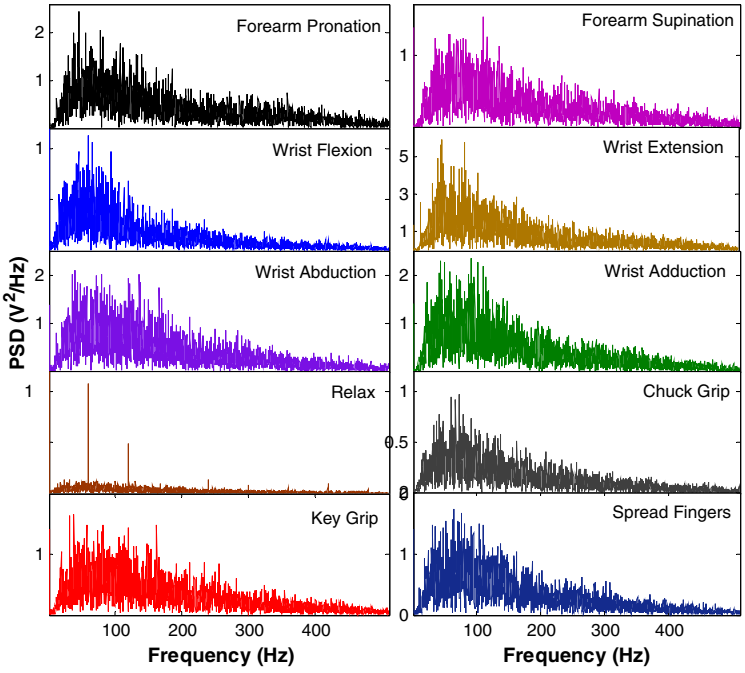

Fig. 2. Power spectrum density (V^2/Hz) of surface EMG signals of 10 hand motions recorded from one of the 16 channels of the data acquisition system.

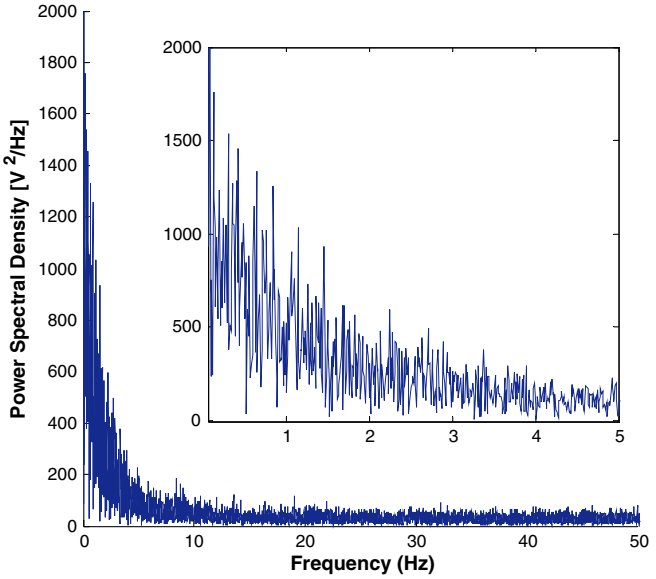

Fig. 3. Power spectrum density (V^2/Hz) of EEG signals recorded from one of the three channels of the data acquisition system.

differences and cognitive-affective state, the underlying constant shape of EEG signals was of primary importance in this study and is not expected to vary between subjects.

2.3. VPA signals

VPA is one of the most common measure for female sexuality and the application of VPA studies is in a broad variety of gynecology, such as female sexual arousal (Laan, Everaerd, & Evers, 1995), sexual function (Rosen et al., 2000), sexual dysfunction (Basson et al., 2004). The vaginal photoplethysmograph monitors the changes in backscattered light in the vaginal canal to reflect sexual arousal (Prause et al., 2005). An embedded light source, usually infrared, generates a light signal that is reflected back to a receiving photocell. The received signal is interpreted as an index of vasoconges-tion, although it is likely to reflect several poorly-characterized physiological processes in the vagina (Prause & Janssen, 2005). The signal pulses with heartbeats, which typically are around 60 BPM in the laboratory, and slow waves concordant with breathing rate are evident in many participants, which may be influenced by vaginal canal length.

Two signals are typically extracted: The first is the DC signal, which provides an index of the total amount of blood. The second is the AC signal, abbreviated as VPA, which reflects phasic changes in the vascular walls that result from pressure changes within the vessels. Both signals have been found to be sensitive to responses to erotic stimulation (Geer, Morokoff, & Greenwood, 1974). However, the construct validity of VPA is better established (Laan et al., 1995) and is used in this study. VPA was collected using the Biopac (Model MP100) data acquisition system. The signal is first band-pass filtered between 0.5 and 30 Hz. The sampling rate was fixed at 80 Hz.

Using PSD, the frequency content of VPA signals are depicted in Fig. 5 for one specific subject. Low-frequency VPA from 20 subjects was recorded in six conditions. Each subject was tested watching a neutral movie followed by an erotic movie with normal blood alcohol levels (BAL), 0.025 BAL, and 0.08 BAL.

3. Mother wavelet selection

Wavelet (Daubechies, 1991) is a capable transform with a flexible resolution in both time- and frequency-domains, which can mainly be divided into discrete and continuous forms; the former is faster because of low computational time, but the continuous type is more efficient and reliable because it maintains all information without down-sampling. Continuous wavelet transform of a signal $s(t) \in L^2(\Re)$ can be defined as

$$CWT(t,\omega) = \left(\frac{\omega}{\omega_0}\right)^{1/2} \int_{-\infty}^{+\infty} s(t')\psi * \left(\frac{\omega}{\omega_0}\right)(t'-t)dt' = \langle s(t), \psi(t)\rangle \quad (1)$$

where $\langle\ \rangle$ means the inner product of the signal and $\psi \in L^2(\Re) \setminus \{0\}$ which is usually termed the mother wavelet function. The mother wavelet function must satisfy the admissibility condition:

$$0 \prec c_\psi = 2\pi \int_{-\infty}^{+\infty} |\hat{\psi}(\xi)|^2 \frac{d\xi}{|\xi|} \prec +\infty \quad (2)$$

and the ratio of ω/ω_0 is the scale factor. The mother wavelet is assumed to be centered at time zero and to oscillate at frequency ω_0. Essentially, Eq. (1) can be interpreted as a decomposition of the signal $s(t')$ into a family of shifted and dilated wavelets $\psi[(\omega/\omega_0)(t'-t)]$. The wavelet basis function $\psi[(\omega/\omega_0)(t'-t)]$ has variable width with consideration to ω at each time t, and is wide for small ω and narrow for large ω. By shifting $\omega(t')$ at fixed parameter ω, the (ω/ω_0)-scale mechanisms in the time response $s(t')$ can be extracted and localized. Alternatively, by dilating $\omega(t')$ at a fixed t, all of the multiscale events of $s(t')$ at t can be analyzed according to the scale parameter (ω/ω_0).

In terms of frequency, low frequencies (high scales) correspond to global information of a signal (that usually spans the entire signal), whereas high frequencies (low scales) correspond to detailed information. In small scales, a temporally localized analysis is done; as the scale increases, the breadth of the wavelet function increases, resulting in analysis with less time resolution but greater frequency resolution. The wavelet functions are band-pass in nature, thus partitioning the frequency axis. In fact, a fundamental property of wavelet functions is that $c = \Delta f/f$ where Δf is a measure of the bandwidth, f is the center frequency of the pass-band, and c is a constant. The wavelet functions may therefore be viewed as a bank of analysis filters with a constant relative pass-band.

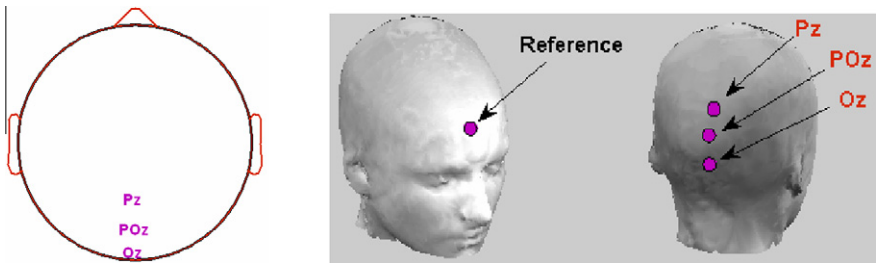

Fig. 4. Channel locations in EEG signals.

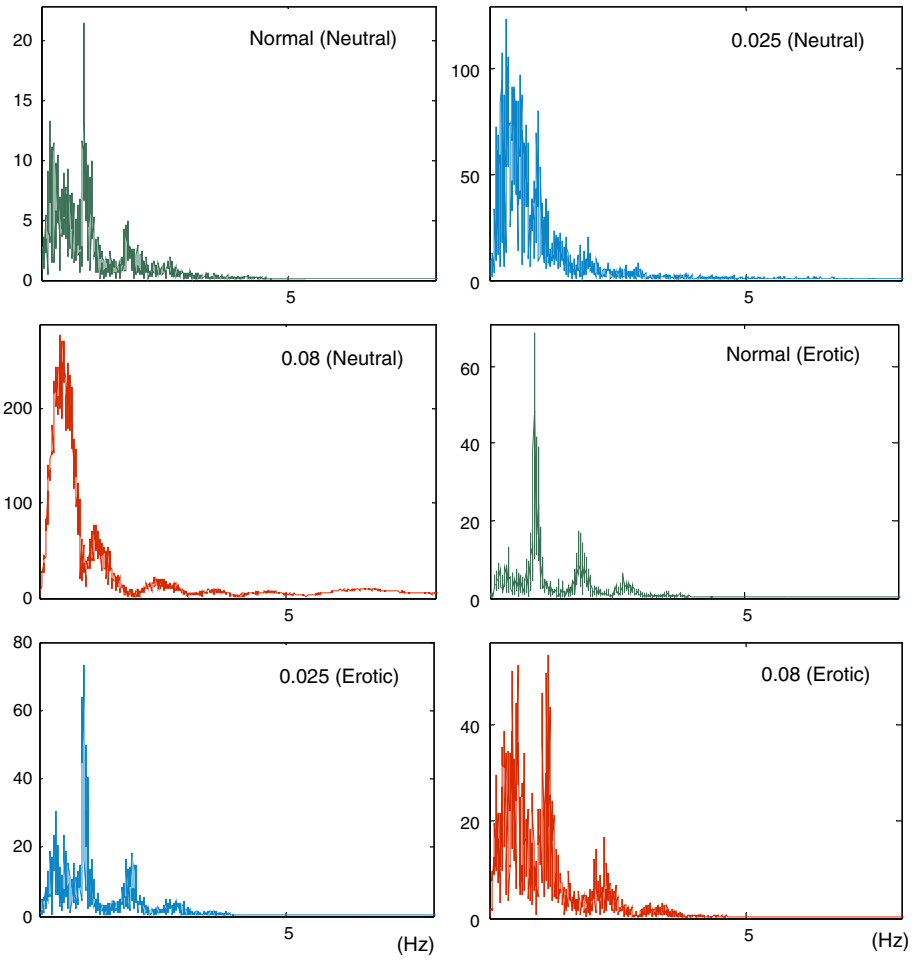

Fig. 5. Power spectrum density (V^2/Hz) of VPA recorded in six classes (one specific subject).

The CWT results in continuous wavelet coefficients (CWC), which illustrate how well a wavelet function *correlates* with a specific signal. If the signal has a major frequency component corresponding to a particular scale, then the wavelet at this scale is similar to the signal at the location where this frequency component occurs, regardless of its amplitudes and phases. Correlation is one of the most common statistical measures, and describes the degree of linear dependence between two variables in terms of a coefficient between −1 and +1. The closer the coefficient is to either −1 or +1, the stronger the correlation between the two variables. The negative or positive sign of the coefficient indicates the direction of the linear dependence. The coefficient 0 implies that the two variables are completely linearly independent of each other. $\rho_{x,y}$, the correlation between two random variables x and y with expected values μ_x and μ_y and standard deviations σ_x and σ_y is defined as:

$$\rho_{x,y} = \frac{\mathrm{cov}(x,y)}{\sigma_x \sigma_y} = \frac{E((x-\mu_x)(y-\mu_y))}{\sigma_x \sigma_y}, \tag{3}$$

where E stands for expected value of the variable and cov stands for covariance. As $E(x) = \mu_x$, $E(y) = \mu_y$ and $\sigma^2(x) = E(x^2) - E^2(x)$, $\sigma^2(y) = E(y^2) - E^2(y)$, $\rho_{x,y}$ can be defined as:

$$\rho_{x,y} = \frac{E(xy) - E(x)E(y)}{\sqrt{E(x^2) - E^2(x)}\sqrt{E(y^2) - E^2(y)}} \tag{4}$$

In this research, the outcome of the correlation between signal and wavelet basis function (CWC) has been established as the basis for comparing selected mother wavelet functions. Consequently, to find the most similar mother wavelet to biosignals, mother wavelets from different families including Haar, Daubechies (db), Symlet, Coiflet, Gaussian, Morlet, complex Morlet, Mexican hat, bio-orthogonal, reverse bio-orthogonal, Meyer, discrete approximation of Meyer, complex Gaussian, Shannon, and frequency B-spline families have been analyzed based on CWC and using the following algorithm:

1. *Signal segmentation:* EMG, EEG, VPA signals were segmented to the 256-points, 500-points, 960-points (12 s) windows, respectively as shown in Figs. 6 and 7 for EMG and VPA.
2. One class of recorded data is selected from one channel for one subject for each type of biosignal. The number of subjects is 20, 6, and 1 for VPA, EMG, and EEG, respectively. There are 1, 16, 6, and 3 channels for recording the signals for VPA, surface EMG, intramuscular EMG, and EEG, respectively.
3. One mother wavelet function is selected from 324 candidates. In the fourth decomposition level, CWC of the segmented signals were calculated (2^4 numbers for each segmented signal).
4. Absolute value of CWC in each scale (2^4 scales) was determined using 324 mother wavelets in a segmented signal for each of the 10 hand motions for EMG, as well as each of three specific channels for EEG. Next, the sum of this value in all 2^4 scales was determined for 20 EMG segmented signals (signals with the length of 256 points), 50 EEG segmented signals (signals with the length of 500 points), and 15 VPA segmented signals (signals with the length of 960 points). Their average was calculated for each type of signal and called the evaluation criterion (EC) for simplicity and to find the most similar mother

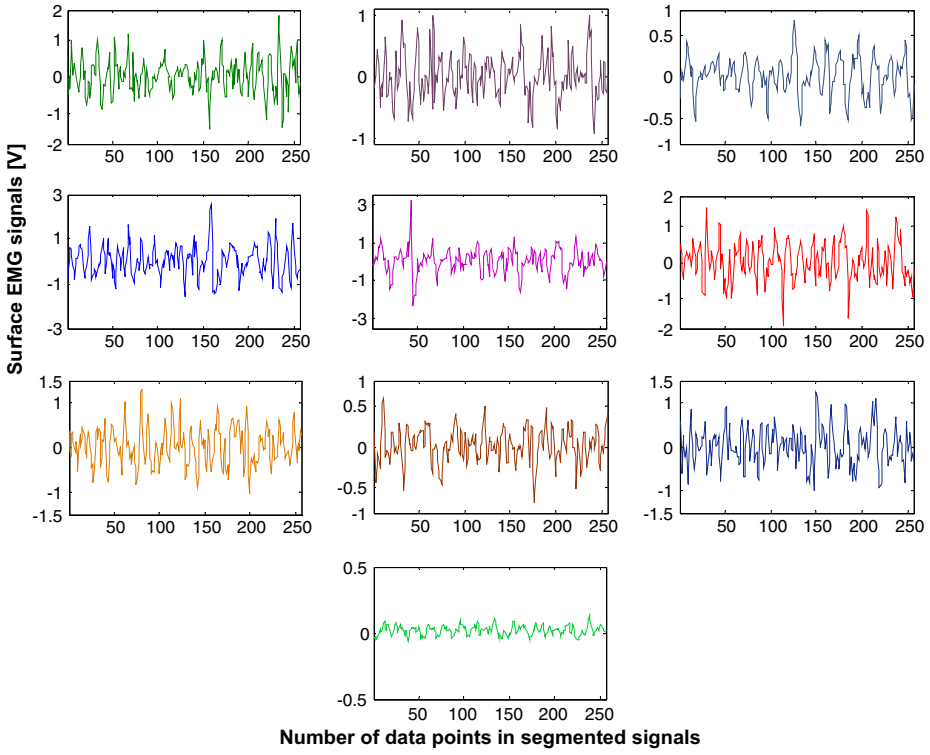

Fig. 6. Segmented surface EMG signals in a 256-points window from one subject performing 10 different hand motions.

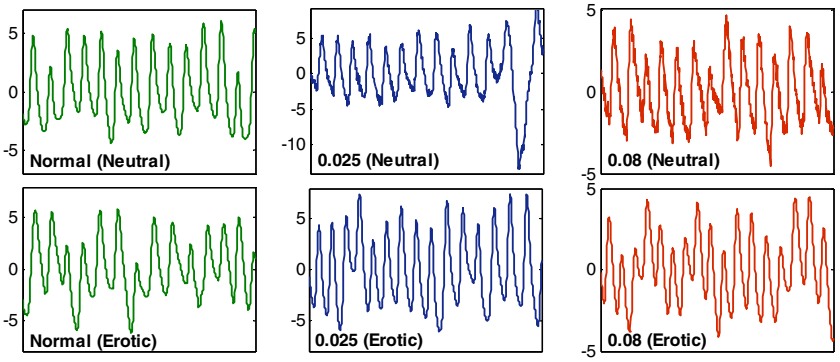

Fig. 7. One segmented VPA in a 960-points window recorded from 6 different classes (*X*-axis equals to 12 s).

function. Fig. 8 shows the decision-making flow chart to determine the most similar mother wavelet function towards biosignals.

5. Steps 2–4 are repeated until all gathered data is analyzed.

In this research, after running the algorithm, the results are shown that from Daubechies family, db44 is the most similar function for all case studies. Daubechies's functions are orthonormal functions. For any integer r, the orthonormal basis function (Daubechies, 1988) for $L^2(\Re)$ will be determined from the following equation:

$$\phi_{r,j,k}(x) = 2^{j/2}\phi_r(2^j - k), \quad j,k \in Z \tag{5}$$

where the function $\varphi_r(x)$ in $L^2(R)$ has the property that $\{\varphi_r(x-k)|k \in Z\}$ is an orthonormal sequence in $L^2(R)$. j is the scaling index, k is the shifting index and r is the filter index.

f_j, at scale 2^{-j}, of a function $f \in L^2(R)$ will be defined as follows:

$$f_j(x) = \sum_k \langle f, \phi_{r,j,k}\rangle \phi_{r,j,k}(x). \tag{6}$$

The details or fluctuations are determined by:

$$d_j(x) = f_{j+1}(x) - f_j(x). \tag{7}$$

To analyze these details at a certain scale, the orthonormal basis function, ψ_r, with similar characteristics to those of above-mentioned $\varphi_r(x)$ has been defined. $\varphi_r(x)$ and $\psi_r(x)$, called the father wavelet and the mother wavelet functions, respectively, are the wavelet prototype functions required by the wavelet analysis. Wavelets such as those defined in Eq. (5) are generated from the father or the mother wavelet by changing scale and translation in time (Liang & Que, 2009).

Daubechies' orthonormal basis has the following characteristics:

- ω_r has the compact support interval $[0, 2r+1]$.
- ω_r has about $r/5$ continuous derivatives.

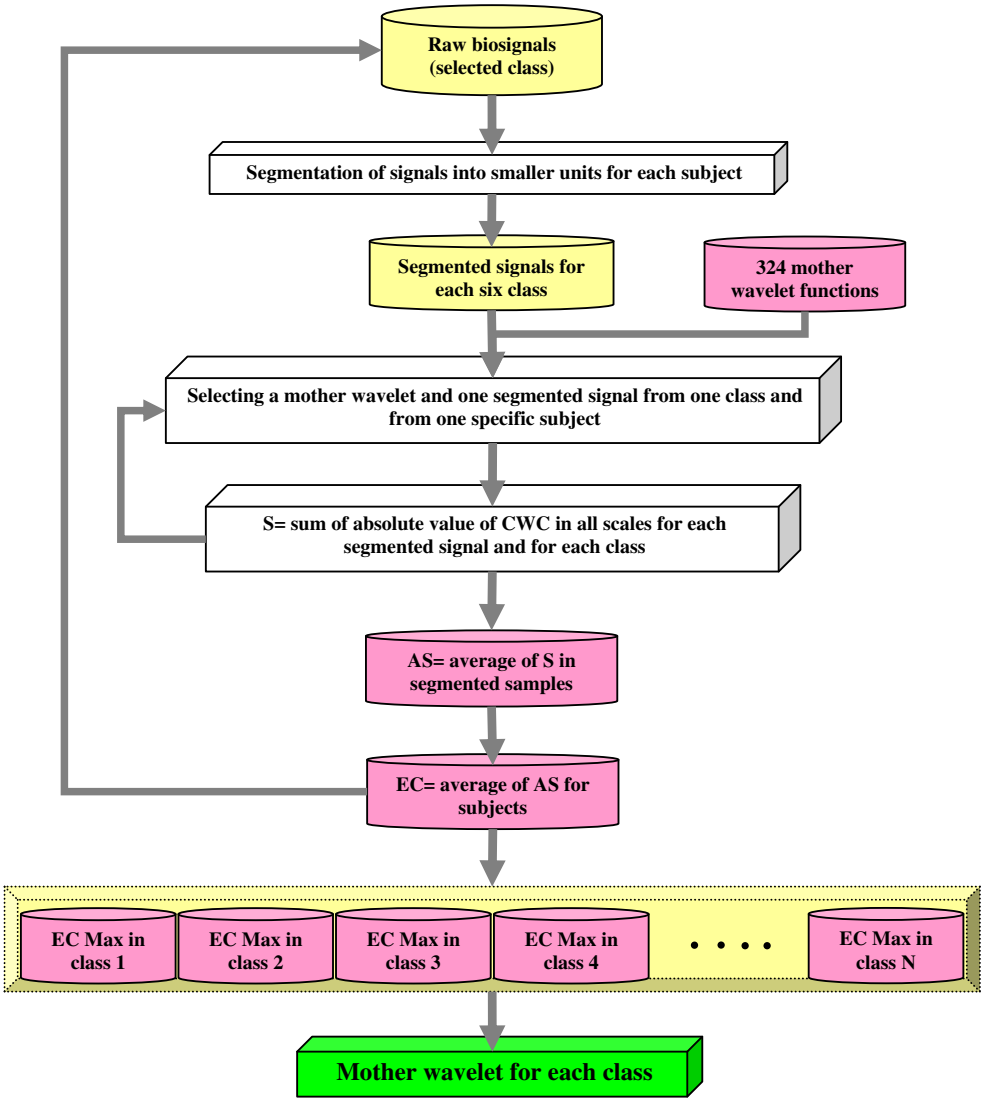

Fig. 8. Searching algorithm to find the most similar mother wavelet based on evaluation criterion (for biosignals).

- $\int_{-\infty}^{\infty} \psi_r(x)dx = \int_{-\infty}^{\infty} x^r \psi_r(x)dx = 0.$

Daubechies' wavelets provide appropriate results in signal processing techniques due to the above-mentioned properties. A wavelet function with compact support can be implemented easily by finite length filters. Moreover, the compact support enables spatial domain localization. Since the wavelet basis functions have continuous derivatives, they decompose a continuous function more efficiently while avoiding edge artifacts. Since the mother wavelets are used to characterize details in a signal, they should have a zero integral so that the trend information is stored in the coefficients obtained by the father wavelet. A Daubechies' wavelet representation of a function is a linear combination of the wavelet basis functions. Daubechies' wavelet transforms are usually implemented numerically via quadratic mirror filters. Multiresolution analysis of the trend and fluctuation of a function is implemented by convolving it with a low-pass filter and a high-pass filter that are versions of the same wavelet.

As shown in biosignals, the signal with a sharp spike is properly analyzed by Daubechies' wavelets, because much less energy (or trend) is stored in the high-pass bands. Hence, Daubechies' wavelets are ideally suited for natural signals. In general, Daubechies' wavelets with long-length filters give more appropriate energy concentration than those with short-length filters. Therefore, the mentioned reason supports the use of EC to find the most similar function to biosignals. Besides, as illustrated in Fig. 9, db44 is the only Daubechies function with near-symmetric characteristic as well as having sharp spike that would be matched with natural signals.

4. Results and discussion

The result shows that, among all wavelet families considered in Tables 1A–2B (Appendix A), Daubechies 44 (db 44) provides a better fit to the tested biosignals. Figs. 10–12 show the EC across mother wavelet candidates for surface EMG, EEG, and VPA signals, respectively. For example, in Fig. 10, all classes of EMG (for 10 different hand motions) have a peak whose amplitude is greater than those calculated by the other candidate mother wavelets. The peak represents the largest EC which is calculated by db44. The same pattern was achieved for other biosignals. The difference between db44 and the other 323 wavelet functions towards biosignals is

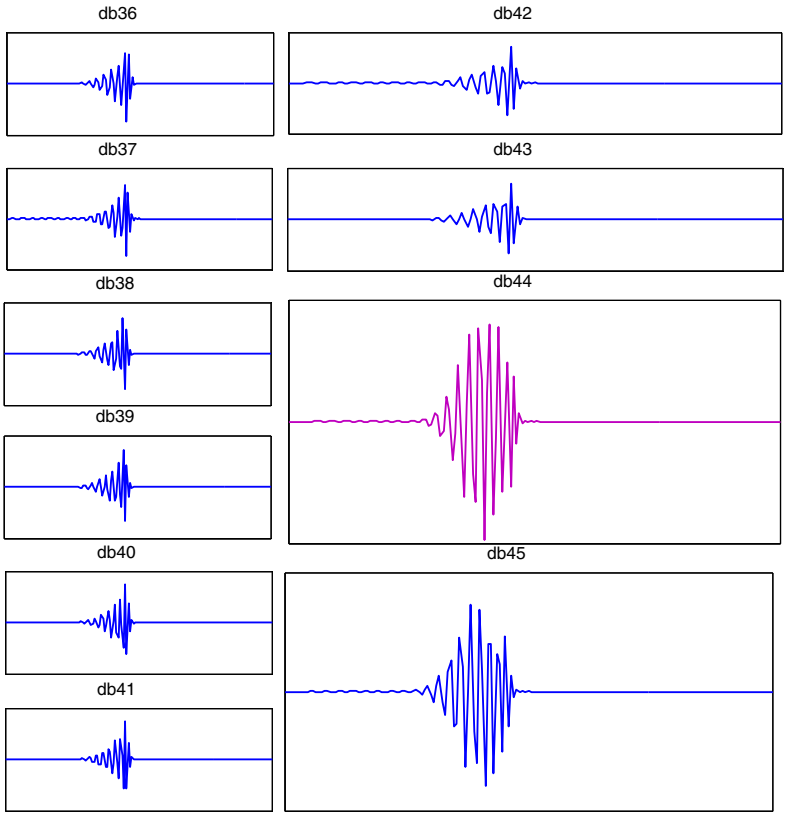

Fig. 9. High-order Daubechies functions.

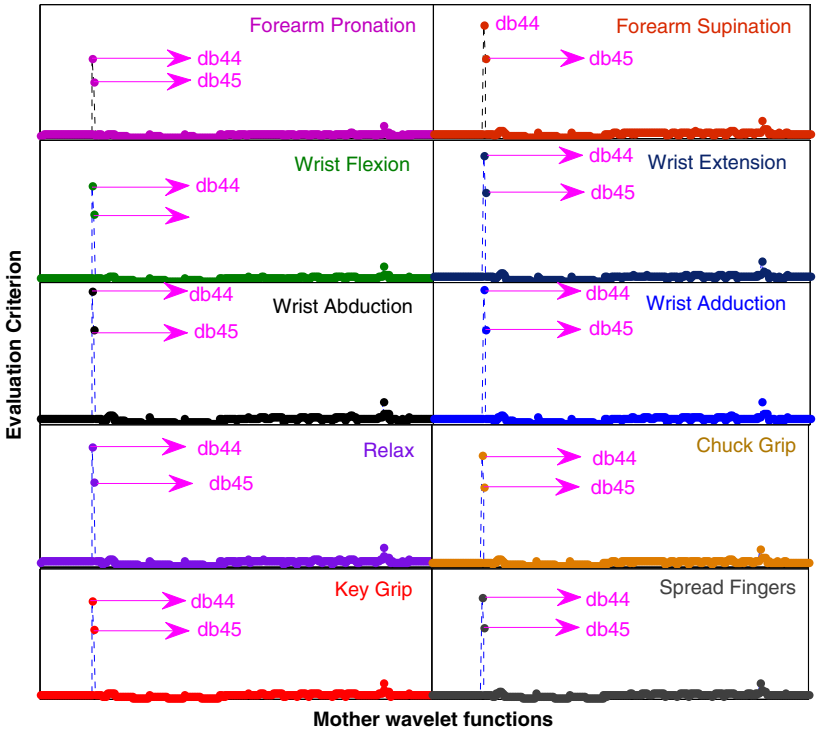

Fig. 10. Evaluation criterion (no unit) across mother wavelet candidate for surface EMG signals recorded from one channels of data acquisition system for 10 hand motions.

noticeable. This would be due to the shape of db functions, which do not change dramatically in low-order Daubechies. Therefore, low order Daubechies have similar performance to the biosignal. However, in higher order, the difference of functions' shape between two adjacent db functions is more distinct (see Fig. 9). In Fig. 13, the trend of Daubechies family and EC was magnified for

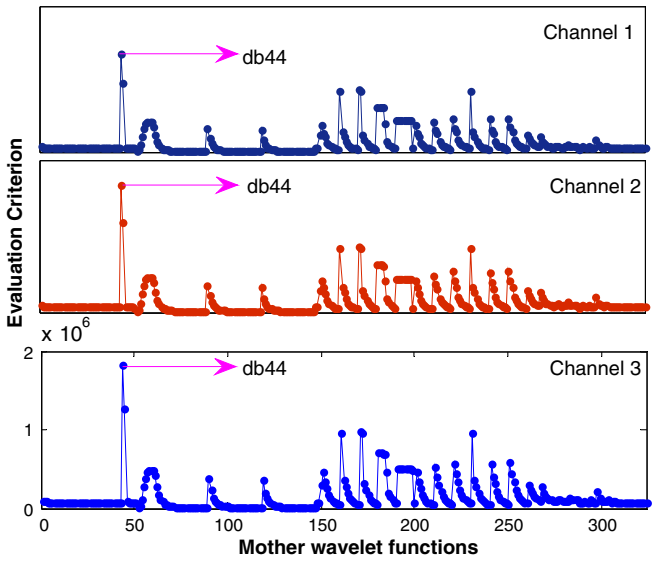

Fig. 11. Evaluation criterion (no unit) across 324 mother wavelet candidates for EEG signals across three channels (Pz, POz, Oz).

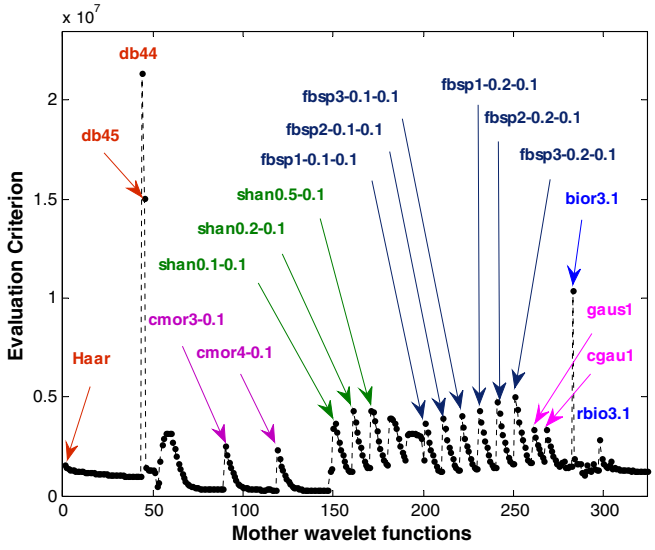

Fig. 12. Evaluation criterion (no unit) vs. mother wavelets for VPA signals recorded from one subject.

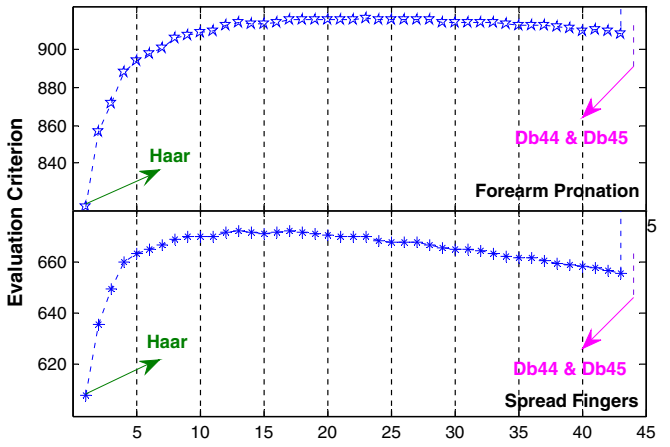

Fig. 13. Trend of Daubechies family vs. evaluation criterion in Intramuscular EMG signals for two motions.

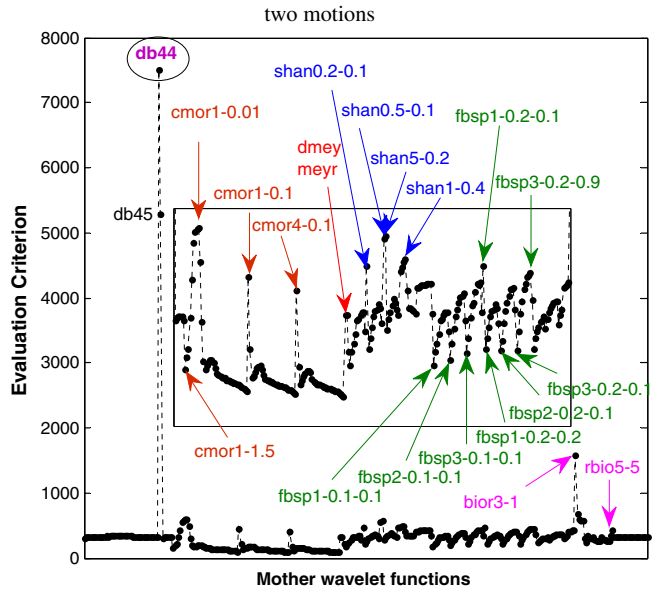

Fig. 14. Evaluation criterion (no unit) vs. mother wavelets for intramuscular EMG signals recorded from one of the six channels of data acquisition system.

Intramuscular EMG signals. As shown, the EC increases slightly in low-order db and decreases slightly for high-order db. This demonstrates that Daubechies functions do not behave dramatically different on the biosignals, while ranging from db1 to db43. It also highlights the likely limitation of the mostly lower order Daubechies that typically are used in prior research. The trend changes dramatically for db44, which cannot be seen in Fig. 13 due to scaling restrictions.

db44 and db45 are the most similar functions as the other 322 functions have pronouncedly poorer performance (similarity). Closer examination of the evaluation criterion (see Figs. 12 and 14) for VPA and intramuscular EMG reveals some variability of fit amongst other function families. To demonstrate the difference between db44 and the other functions, the continuous wavelet coefficients of one of the segmented unit signals using db44 has been compared to those calculated with the Morlet function, which has been used frequently in previous research (see Figs. 15 and 16, see Fig. 17 for decomposition scale) (e.g. Saravanan, Kumar Siddabattuni, & Ramachandran, 2008). The difference between the values of the CWC (*Y*-axis) calculated by db44 is much higher than those calculated by Morlet function. Moreover, periodic sinusoidal trends also are obvious using the db44. This is a very desirable feature, because it means that periodic behavior can be extracted from biological signals using db44 function. This might be useful for preprocessing biological signals.

Some other complex mother wavelets (in addition to db44 and db45) show high similarity to EEG and VPA signals (e.g. see Fig. 12). After db44 and db45, EEG signals also display some similarity to bior 3.1 and other complex mother wavelets unlike the EMG. However, these differences appear minor and appear due mostly to complex functions with different wavelet center frequency. The center frequency varies simply with the frequency contents of the signals.

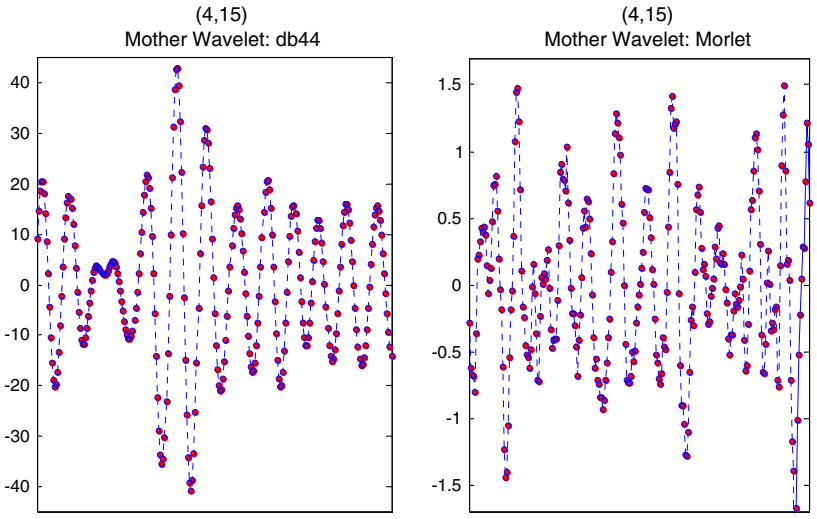

Fig. 15. CWC of a segmented surface EMG signal calculated using Morlet and Db44 in one specific scale. (Title: scale – see Fig. 17).

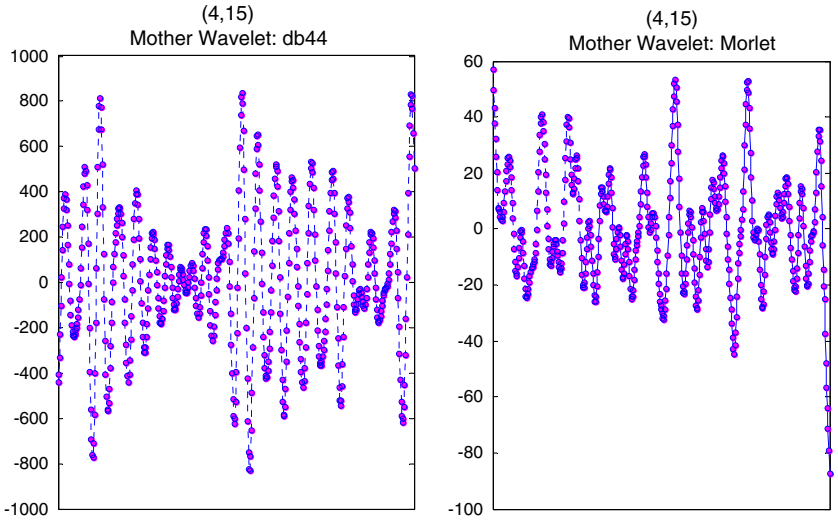

Fig. 16. CWC of a segmented EEG signal calculated using Morlet and Db44 in one specific scale. (Title: scale – see Fig. 17).

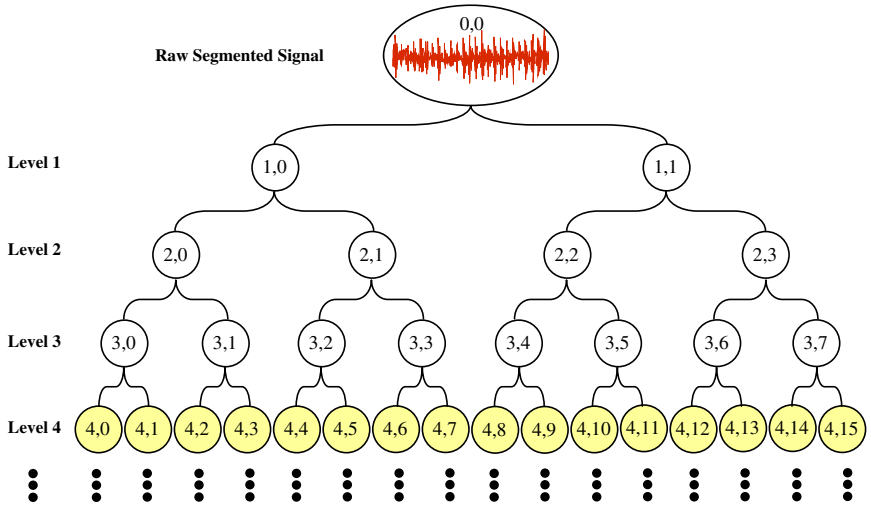

Fig. 17. Decomposition tree and the level of decomposition (Rafiee et al., 2010).

Table 1A
Studied wavelet families in this research (Rafiee et al., 2010).

No.	Family (short form)	Order
1	Haar (db1)	db 1
2–45	Daubechies(db)	db 2–db 45
46–50	Coiflet (coif)	coif 1–coif 5
51	Morlet (Morl)	morl
52–147	Complex Morlet (cmor Fb-Fc)[a]	Included Table 1B
148	Discrete Meyer (dmey)	dmey
149	Meyer (meyr)	meyr
150	Mexican Hat (mexh)	mexh
151–200	Shannon (Shan Fb-Fc)[a]	Included Table 1B
201–260	Frequency B-Spline (fbsp M-Fb- Fc)[a]	Included Table 1B
261–267	Gaussian (gaus)	gaus 1–gaus 7
268–275	Complex Gaussian (cgau)	cgau 1–cgau 8
276–290	Biorthogonal (bior Nr.Nd)[b]	Included Table 1B
291–305	Reverse Biorthogonal (rbio Nr.Nd)[b]	Included Table 1B
306–324	Symlet (sym)	sym 2–sym 20

[a] Fb is a bandwidth parameter, Fc is a wavelet center frequency, and M is an integer order parameter.
[b] Nr and Nd are orders: r for reconstruction/d for decomposition.

5. Conclusions

In summary, db44 appears to be the most similar function to EMG, EEG, and VPA signals among 324 mother wavelet functions. Symmetric mother wavelets have been shown more proper results with biosignals in prior research. Daubechies are orthogonal compact support functions and are not symmetric. However, db44 possesses a near-symmetric attribute (see Fig. 9) that well-matched the biosignals. Most biosignals possess sharp spikes that could be appropriately analyzed using Daubechies' wavelets to reflect sharp, asymmetric spikes seen in these signals. These features of db44 suggest that it would be effective for many biosignal processing methods based on the resemblance of the signal and mother wavelet function.

The similarity between signal and mother wavelet function is not always proper for signal processing based on wavelet transform and it is just appropriate for those wavelet-based processing methods based on the resemblance between signals and mother functions.

Table 1B
Studied wavelet families in detail (Rafiee et al., 2010).

No	Wave	No	Wave	No	Wave	No	Wave	No	Wave
52	1–1.5	100	3–1.1	148	dmey	196	2–0.6	244	2–0.2–0.4
53	1–1	101	3–1.2	149	meyr	197	2–0.7	245	2–0.2–0.5
54	1–0.5	102	3–1.3	150	mexh	198	2–0.8	246	2–0.2–0.6
55	1–0.3	103	3–1.4	151	0.1–0.1	199	2–0.9	247	2–0.2–0.7
56	1–0.2	104	3–1.5	152	0.1–0.2	200	1–1	248	2–0.2–0.8
57	1–0.1	105	3–1.6	153	0.1–0.3	201	1–0.1–0.1	249	2–0.2–0.9
58	1–0.05	106	3–1.8	154	0.1–0.4	202	1–0.1–0.2	250	2–0.2–1
59	1–0.02	107	3–1.9	155	0.1–0.5	203	1–0.1–0.3	251	3–0.2–0.1
60	1–0.01	108	3–2	156	0.1–0.6	204	1–0.1–0.4	252	3–0.2–0.2
61	2–0.1	109	3–2.1	157	0.1–0.7	205	1–0.1–0.5	253	3–0.2–0.3
62	2–0.2	110	3–2.2	158	0.1–0.8	206	1–0.1–0.6	254	3–0.2–0.4
63	2–0.3	111	3–2.3	159	0.1–0.9	207	1–0.1–0.7	255	3–0.2–0.5
64	2–0.4	112	3–2.4	160	0.1–1	208	1–0.1–0.8	256	3–0.2–0.6
65	2–0.5	113	3–2.5	161	0.2–0.1	209	1–0.1–0.9	257	3–0.2–0.7
66	2–0.6	114	3–2.6	162	0.2–0.2	210	1–0.1–1	258	3–0.2–0.8
67	2–0.7	115	3–2.7	163	0.2–0.3	211	2–0.1–0.1	259	3–0.2–0.9
68	2–0.8	116	3–2.8	164	0.2–0.4	212	2–0.1–0.2	260	3–0.2–1
69	2–0.9	117	3–2.9	165	0.2–0.5	213	2–0.1–0.3	276	1.1
70	2–1	118	3–3	166	0.2–0.6	214	2–0.1–0.4	277	1.3
71	2–1.1	119	4–0.1	167	0.2–0.7	215	2–0.1–0.5	278	1.5
72	2–1.2	120	4–0.2	168	0.2–0.8	216	2–0.1–0.6	279	2.2
73	2–1.3	121	4–0.3	169	0.2–0.9	217	2–0.1–0.7	280	2.4
74	2–1.4	122	4–0.4	170	0.2–1	218	2–0.1–0.8	281	2.6
75	2–1.5	123	4–0.5	171	0.5–0.1	219	2–0.1–0.9	282	2.8
76	2–1.6	124	4–0.6	172	0.5–0.2	220	2–0.1–1	283	3.1
77	2–1.8	125	4–0.7	173	0.5–0.3	221	3–0.1–0.1	284	3.3
78	2–1.9	126	4–0.8	174	0.5–0.4	222	3–0.1–0.2	285	3.5
79	2–2	127	4–0.9	175	0.5–0.5	223	3–0.1–0.3	286	3.7
80	2–2.1	128	4–1	176	0.5–0.6	224	3–0.1–0.4	287	3.9
81	2–2.2	129	4–1.1	177	0.5–0.7	225	3–0.1–0.5	288	4.4
82	2–2.3	130	4–1.2	178	0.5–0.8	226	3–0.1–0.6	289	5.5
83	2–2.4	131	4–1.3	179	0.5–0.9	227	3–0.1–0.7	290	6.8
84	2–2.5	132	4–1.4	180	0.5–1	228	3–0.1–0.8	291	1.1
85	2–2.6	133	4–1.5	181	1–0.1	229	3–0.1–0.9	292	1.3
86	2–2.7	134	4–1.6	182	1–0.2	230	3–0.1–1	293	1.5
87	2–2.8	135	4–1.8	183	1–0.3	231	1–0.2–0.1	294	2.2
88	2–2.9	136	4–1.9	184	1–0.4	232	1–0.2–0.2	295	2.4
89	2–3	137	4–2	185	1–0.5	233	1–0.2–0.3	296	2.6
90	3–0.1	138	4–2.1	186	1–0.6	234	1–0.2–0.4	297	2.8
91	3–0.2	139	4–2.2	187	1–0.7	235	1–0.2–0.5	298	3.1
92	3–0.3	140	4–2.3	188	1–0.8	236	1–0.2–0.6	299	3.3
93	3–0.4	141	4–2.4	189	1–0.9	237	1–0.2–0.7	300	3.5
94	3–0.5	142	4–2.5	190	1–1	238	1–0.2–0.8	301	3.7
95	3–0.6	143	4–2.6	191	2–0.1	239	1–0.2–0.9	302	3.9
96	3–0.7	144	4–2.7	192	2–0.2	240	1–0.2–1	303	4.4
97	3–0.8	145	4–2.8	193	2–0.3	241	2–0.2–0.1	304	5.5
98	3–0.9	146	4–2.9	194	2–0.4	242	2–0.2–0.2	305	6.8
99	3–1	147	4–3	195	2–0.5	243	2–0.2–0.3		

Table 2A
Wavelet families and their specifications.

Property	Haar	Db	Coif	Morl	Cmor	Dmey	Meyr	Mexh
Continuous wavelet transform	✓	✓	✓	✓		✓	✓	✓
Discrete wavelet transform	✓	✓	✓			✓	✓	
Complex CWT					✓			
Compact supported orthogonal	✓	✓	✓					
Compact supported biorthogonal								
Orthogonal analysis	✓	✓	✓				✓	
Biorthogonal analysis	✓	✓	✓				✓	
Symmetry				✓	✓	✓	✓	✓
Near symmetry			✓					
Asymmetry	✓	✓						
Explicit expression	✓			✓	✓			✓

Table 2B
Wavelet families and their specifications.

Property	Shan	Fbsp	Gaus	Cgau	Bior	Rbio	Sym
Continuous wavelet transform			✓		✓	✓	✓
Discrete wavelet transform					✓	✓	✓
Complex CWT	✓	✓		✓			
Compact supported orthogonal							✓
Compact supported biorthogonal					✓	✓	
Orthogonal analysis							✓
Biorthogonal analysis					✓	✓	✓
Symmetry	✓	✓	✓	✓	✓	✓	
Near symmetry							✓
Asymmetry							
Explicit expression	✓	✓	✓	✓	For splines	For splines	

Acknowledgments

The authors are thankful to Professor Kevin Englehart, associate director of the Institute of Biomedical Engineering at the University of New Brunswick in Canada, for his supporting us with experimental EMG signals used in this research. The authors also acknowledge funding support from the US DARPA (Award No.: W81XWH-07-2-0078) for Idaho State University Smart Prosthetic Hand Technology – Phase I.

Appendix A

See Tables 1A–2B.

References

Antonino-Daviu, J. A., Riera-Guasp, M., Folch, J. R., & Palomares, M. P. M. (2006). Validation of a new method for the diagnosis of rotor bar failures via wavelet transform in industrial induction machines. *IEEE Transactions on Industry Applications, 42*(4).

Asghari Oskoei, M., & Hu, H. (2007). Myoelectric control systems—A survey. *Biomedical Signal Processing and Control, 2*, 275–294.

Basson, R., Althof, S., Davis, S., Fugl-Meyer, K., Goldstein, I., Leiblum, S., et al. (2004). Summary of the recommendations on sexual dysfunctions in women. *The Journal of Sexual Medicine, 1*(1), 24–34.

Brechet, L., Lucas, M. F., Doncarli, C., & Farina, D. (2007). Compression of biomedical signals with mother wavelet optimization and best-basis wavelet packet selection. *IEEE Transactions on Biomedical Engineering, 54*(12).

Daubechies, I. (1988). Orthonormal bases of compactly supported wavelets. *Communications on Pure and Applied Mathematics, 41*, 909–996.

Daubechies, I. (1991). Ten lectures on wavelets. CBMS-NSF series in applied mathematics (SIAM).

Engin, M., Fedakar, M., Engin, E. Z., & Korűrek, M. (2007). Feature measurements of ECG beats based on statistical classifiers. *Measurement: Journal of the International Measurement Confederation, 40*(9–10), 904–912.

Englehart, K., Hudgins, B., & Parker, P. A. (2001). A wavelet-based continuous classification scheme for multifunction myoelectric control. *IEEE Transactions on Biomedical Engineering, 48*(3), 302–311.

Farina, D., do Nascimento, O. F., Lucas, M. F., & Doncarli, C. (2007). Optimization of wavelets for classification of movement-related cortical potentials generated by variation of force-related parameters. *Journal of Neuroscience Methods*(162), 357–363.

Farina, D., Lucas, M. F., & Doncarli, C. (2008). Optimized wavelets for blind separation of non-stationary surface myoelectric signals. *IEEE Transactions on Biomedical Engineering, 55*(1).

Flanders, M. (2002). Choosing a wavelet for single-trial EMG. *Journal of Neuroscience Methods*(116), 165–177.

Geer, J. H., Morokoff, P., & Greenwood, P. (1974). Sexualarousal in women: The development of a measurement device for vaginal blood volume. *Archives of Sexual Behavior, 3*, 559–564.

Hargrove, L. J., Englehart, K., & Hudgins, B. (2007). A comparison of surface and intramuscular myoelectric signal classification. *IEEE Transactions on Biomedical Engineering, 54*(5).

Hermens, H., Freriks, B., Merletti, R., Stegeman, D., Blok, J., Rau, G., et al. (1999). *European recommendations for surface electromyography*. RRD Publisher.

Kurt, M. B., Sezgin, N., Akin, M., Kirbas, G., & Bayram, M. (2009). The ANN-based computing of drowsy level. *Expert Systems with Applications, 36*(2 Part 1), 2534–2542.

Laan, E., Everaerd, W., & Evers, A. (1995). Assessment of female sexual arousal: Response specificity and construct validity. *Psychophysiology, 32*, 476–485.

Landolsi, T. (2006). Accuracy of the split-step wavelet method using various wavelet families in simulating optical pulse propagation. *Journal of the Franklin Institute*(343), 458–467.

Liang, W., & Que, P.-W. (2009). Optimal scale wavelet transform for the identification of weak ultrasonic signals. *Measurement: Journal of the International Measurement Confederation, 42*(1), 164–169.

Lucas, M. F., Gaufriau, A., Pascual, S., Doncarli, C., & Farina, D. (2008). Multi-channel surface EMG classification using support vector machines and signal-based wavelet optimization. *Biomedical Signal Processing and Control*(3), 169–174.

Manikandan, M. S., & Dandapat, S. (2008). Wavelet threshold based TDL and TDR algorithms for real-time ECG signal compression. *Biomedical Signal Processing and Control, 3*(2008), 44–66.

Prause, N., & Janssen, E. (2005). Blood flow: vaginal photoplethysmography. In I. Goldstein, C. M. Meston, S. Davis, & A. Traish (Eds.), *Textbook of female sexual dysfunction*. London: Taylor & Francis Medical Books.

Prause, N., Janssen, E., & Hetrick, W. (2007). Attention and emotional responses to sexual stimuli and their relationship to sexual desire. *Archives of Sexual Behavior, 37*(6), 934–949.

Rafiee, J., Rafiee, M. A., Yavari, F., & Schoen, M. P. (2010). Feature extraction of forearm EMG signals for prosthetics. *Expert System with Applications*. doi:10.1016/j.eswa.2010.09.068.

Rafiee, J., Rafiee, M. A., & Michaelsen, D. (2009). Female sexual responses using signal processing techniques. *Journal of Sexual Medicine, 6*(11).

Rafiee, J., & Tse, P. W. (2009). Use of autocorrelation in wavelet coefficients for fault diagnosis. *Mechanical Systems and Signal Processing, 23*, 1554–1572.

Rosen, R., Brown, C., Heiman, J., Leiblum, S., Meston, C., Shabsigh, R., et al. (2000). The female sexual function index (FSFI): A multidimensional self-report instrument for the assessment of female sexual function. *Journal of Sex and Marital Therapy, 26*(2), 191–208.

Rosso, O. A., Blanco, S., Yordanova, J., Kolev, V., Figliola, A., Schürmann, M., et al. (2001). Wavelet entropy: A new tool for analysis of short duration brain electrical signals. *Journal of Neuroscience Methods, 105*(1), 65–75.

Saravanan, N., Kumar Siddabattuni, V. N. S., & Ramachandran, K. I. (2008). A comparative study on classification of features by SVM and PSVM extracted using Morlet wavelet for fault diagnosis of spur bevel gearbox. *Expert Systems with Applications, 35*(3), 1351–1366.

Singh, B. N., & Tiwari, A. K. (2006). Optimal selection of wavelet basis function applied to ECG signal denoising. *Digital Signal Processing*(16), 275–287.

Subasi, A. (2005). Automatic recognition of alertness level from EEG by using neural network and wavelet coefficients. *Expert Systems with Applications, 28*(4), 701–711.

Ting, W., Guo-Zheng, Y., Bang-Hua, Y., & Hong, S. (2008). EEG feature extraction based on wavelet packet decomposition for brain computer interface. *Measurement: Journal of the International Measurement Confederation, 41*(6), 618–625.

Tse, P. W., Yang, W. X., & Tam, H. Y. (2004). Machine fault diagnosis through an effective exact wavelet analysis. *Journal of Sound and Vibration*(277), 1005–1024.